MOLTEN SALT SEPARATION FROM URANIUM DURING THE PROCESSING OF SPENT NUCLEAR FUEL

B.R. Westphal, J.R. Krsul, and D.W. Maddison
Argonne National Laboratory
P.O. Box 2528
Idaho Falls, Idaho 83403

Abstract

As part of the spent fuel treatment program at Argonne National Laboratory, a vacuum distillation process is being employed for the recovery of uranium following an electrorefining process. Distillation of a molten salt electrolyte, primarily consisting of a eutectic mixture of lithium and potassium chlorides with minor amounts of fission product chlorides, from uranium is achieved by a batch operation called cathode processing. The degree of molten salt separation from uranium at the cathode processor is termed distillation efficiency. This paper discusses the efficiency of the cathode processor via the use of representative isotopic tracers of the fission product chlorides. The relationship between distillation efficiencies, chloride vapor pressures, and relative concentrations is also discussed and applied to other chloride species of the system.

Introduction

The electrometallurgical treatment of Experimental Breeder Reactor-II (EBR-II) spent nuclear fuel at Argonne National Laboratory comprises a set of operations designed to produce a low enriched uranium ingot for disposition or reuse [1-2]. Electrometallurgical treatment of EBR-II spent fuel has distinct advantages over other processing technologies in that the bond sodium, used for heat transfer purposes during reactor operations, poses no problems to the process in addition to being neutralized. Metallic uranium is initially separated by an electrorefining operation although additional recoveries are realized by a distillation process [3-4]. Treatment of the EBR-II spent fuel was initiated in June 1996 and continues currently on the balance of the spent fuels.

Spent fuel treatment is performed in the Fuel Conditioning Facility (FCF) located in Idaho. The fuel is either dismantled into elements from assemblies or retrieved directly as elements from storage containers. Initial fuel element handling operations are performed in the air cell of FCF prior to their transfer to the argon cell for element chopping. Elements are chopped into segments by either a solenoid-driven or pneumatic press depending on the fuel type, driver or blanket, respectively. Table I contrasts the two EBR-II fuel types. The segments are then loaded into an anode assembly which contains up to nine perforated baskets depending on the fuel type. The anode assembly is installed into the electrorefiner commensurate with the fuel type; Mk-IV for driver and Mk-V for blanket. Although the two electrorefiner vessels are identical in design, the electrode configurations, liquid contents, and process conditions are different. Electrorefining is performed by transporting uranium from the loaded anode baskets to a cathodic surface. The anodes are submerged in a molten lithium chloride – potassium chloride (LiCl-KCl) electrolyte for dissolution of the uranium and fission products. The cathode products from both electrorefiners are primarily uranium metal coated with the eutectic LiCl-KCl salt and fission product chlorides. Final recovery of the uranium in the cathode product is achieved by distilling the salt in a cathode processor by vacuum retort. A casting step following distillation allows for isotopic dilution and sampling of the uranium products.

Table I. EBR-II Spent Fuel Compositions (wt. %)

Constituent	Driver	Blanket
Uranium	81.3	98.4
Zirconium	9.7	0.0
Sodium	2.1	0.6
Fission Products	6.4	0.1
Transuranics	0.5	0.9

The cathode processor (Figure 1) is an induction-heated furnace capable of temperatures to 1400°C and vacuums to less than 0.1 Torr. The furnace region contains a passively cooled induction coil and a graphite furnace liner that acts as the susceptor to heat the process materials. Removal of the chloride salts from the uranium in the cathode processor is accomplished by reducing the

internal pressure to less than 1 Torr and heating to 1200°C. Following the separation of the molten salts from uranium, the consolidated uranium ingot is further processed in the casting furnace where samples are taken for chemical analyses. More specific details of the cathode processor operations are given elsewhere [4-5].

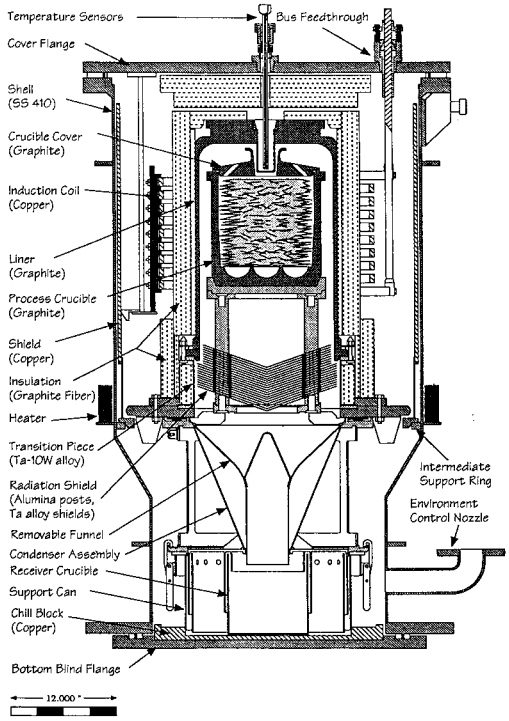

Figure 1: Schematic of cathode processor equipment.

Background

Since the concentrations of salt constituents in the uranium product are below the detection capabilities of standard analytical techniques, i.e. Inductively Coupled Plasma – Atomic Emission Spectroscopy, it is difficult to assess the efficiency of distillation in the cathode processor. Based on the standard techniques, the separation of chloride salts from uranium appears to be 100% efficient. However, when gamma-ray spectroscopy is employed, the detection of concentrations into the trace quantity regime is possible and efficiencies of less than 100% can be calculated.

Gamma-ray spectroscopy not only has the advantage of being able to detect several active species simultaneously but also of detecting those species to extremely sensitive levels [6]. Particular radioactive nuclides can be determined quantitatively given that their gamma emissions are sufficient for detection. It is for this reason that radioactive tracers are commonly used to represent elements or compounds in certain applications where the detection of the element or compound would otherwise be impossible. Of course, this assumes that the chemical behavior of the radioactive nuclide is the same as that of the element or compound.

Of the radioactive nuclides routinely detected by gamma spectroscopy in the uranium product samples, the isotopes of cesium (Cs), cerium (Ce), and europium (Eu) are of particular interest since they represent the salt species of cesium chloride (CsCl), cerium trichloride ($CeCl_3$), and europium dichloride ($EuCl_2$), see Table II. The initial investigation into the efficiency of the cathode processor misidentified the europium chloride species as europium trichloride ($EuCl_3$) instead of $EuCl_2$ [7]. Although both oxidation states for europium have been observed, the divalent state would seem the most probable given their electron configurations [8-9].

Table II. Representative Species for Radioactive Isotopes

Element	Salt Compound	Radioactive Isotope
Cs	CsCl	Cs-134, 137
Ce	$CeCl_3$	Ce-144
Eu	$EuCl_2$	Eu-154, 155

Given in Figure 2 are the vapor pressure curves for the pure chloride species. Note that the data for $EuCl_2$ are estimated based on ionic radii and similarities with samarium dichloride ($SmCl_2$) [10]. It should also be noted that the range of vapor pressures approximately covers that of all the chloride species in the system.

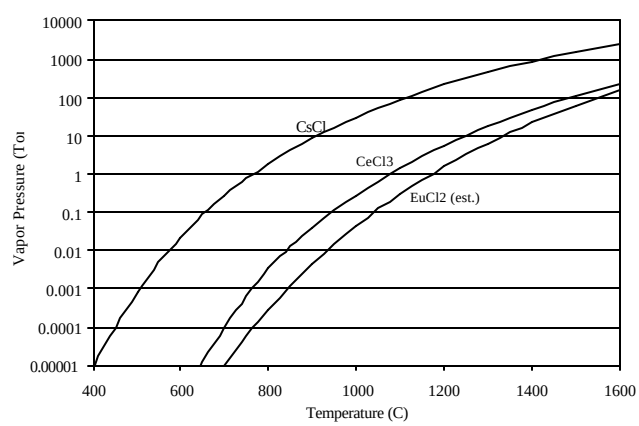

Figure 2: Chloride vapor pressures of Cs, Ce, and Eu.

The elemental fission products Cs, Ce, and Eu, are oxidized to the salt during the dissolution of spent nuclear fuel in the electrorefiner. Due to the significant difference in fission product yields for driver and blanket fuels (Table I), the driver treatment process was chosen for the determination of distillation characteristics in the cathode processor. Shown in Figure 3 are the concentrations of the elemental fission products Cs, Ce, and Eu in the Mk-IV (driver) electrorefiner salt. The concentrations are given versus the number of assemblies processed to date. Cesium is one of the most abundant fission products in the salt while Eu is one of the least.

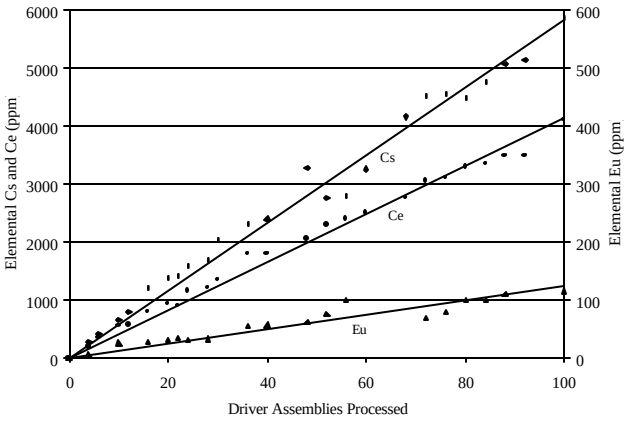

Figure 3: Concentrations of Cs, Ce, and Eu in Mk-IV electrorefiner after 100 assemblies.

Distillation efficiency is defined as the degree of salt separation from uranium in the cathode processor. Knowing the amount of radioactive isotope or tracer in both the product and feed of the cathode processor, the distillation efficiency can be calculated according to:

$$\text{Distillation Efficiency (\%)} = [1 - (\text{Product/Feed})]*100 \qquad (1)$$

Measurement of the tracer in the feed is performed by multiplying the amount of salt adhering to the cathode product, found after cathode processing, by the concentration of the tracer in the Mk-IV electrorefiner salt sample taken after a cathode product. The activity of the tracer in the product is quantified from the sample taken after casting. Distillation effects of the casting process are considered negligible when compared to cathode processing under a vacuum as described previously.

Results and Discussion

The distillation efficiencies for Cs-134, Cs-137, Ce-144, Eu-154, and Eu-155 were calculated for twenty-two batches of driver material processed in the cathode processor. Although the results for Cs-134 and Eu-154 were similar to Cs-137 and Eu-155, respectively, they were limited considering the concentrations of the isotopes. Thus, the distillation efficiencies for Cs-137 and Eu-155 are considered more representatives of elemental Cs and Eu, respectively. Both the feed and product values were adjusted for radioactive decay of the isotopes based on the cathode processor operating date.

The distillation efficiencies for Cs-137, Ce-144, and Eu-155 have been plotted against their concentrations in the Mk-IV electrorefiner salt and are shown in Figures 4, 5, and 6. The efficiencies for all three tracers are greater than 96%, with the Cs-137 and Ce-144 values being considerably higher. Despite the slight scatter in the Eu-155 data, the efficiencies were assumed constant for the concentrations given. If true, this assumption will be validated by a correlation of the individual efficiencies. The constant or averaged distillation efficiencies for Cs-137, Ce-144, and Eu-155 are 99.96%, 99.86%, and 98.61%, respectively.

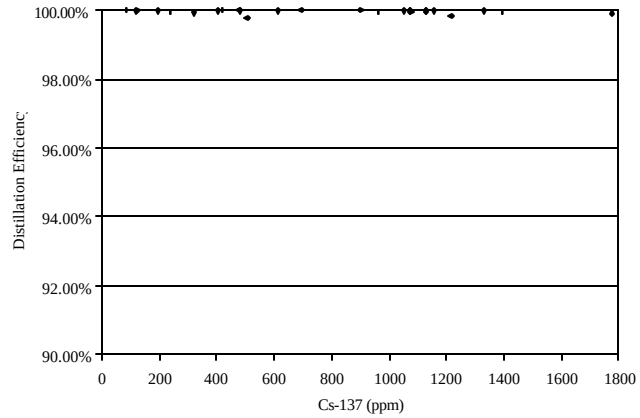

Figure 4: Distillation efficiencies for Cs-137.

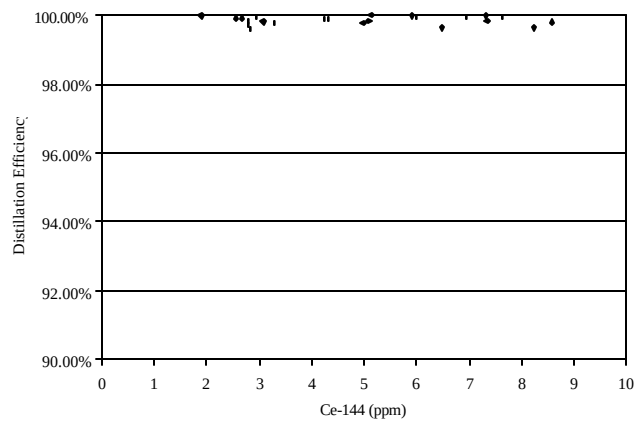

Figure 5: Distillation efficiencies for Ce-144.

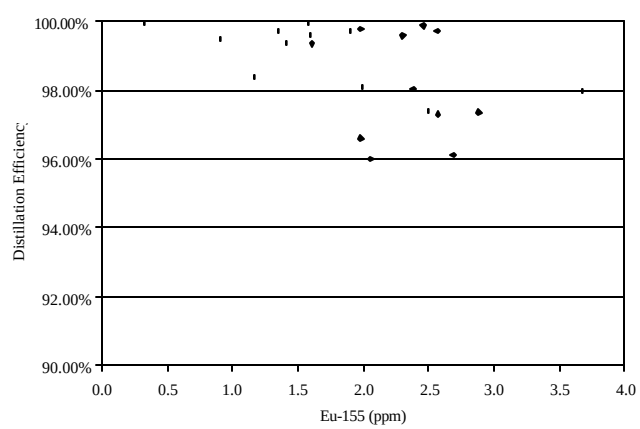

Figure 6: Distillation efficiencies for Eu-155.

Since distillation efficiency is a measure of the salt separation from uranium, the efficiencies of the tracers, which ultimately represent the chloride species, should be related to the vapor pressure or partial pressure of the chloride species in the salt. If Raoult's law is obeyed, the partial pressure of the chloride species in the salt is equal to the concentration or mole fraction of that species in the salt multiplied by the vapor pressure of the pure chloride species. The following equation shows this relationship assuming the solution is ideal:

$$P_i = X_i * P_i^o \qquad (2)$$

Figure 7 depicts distillation efficiencies plotted against the partial pressures of $EuCl_2$, $CeCl_3$, and CsCl in the Mk-IV salt. The partial pressures of $EuCl_2$, $CeCl_3$, and CsCl were calculated from the mole fraction and vapor pressures of pure species. As can be seen, a linear correlation is not evident for the three distillation efficiencies so Raoult's law is not obeyed.

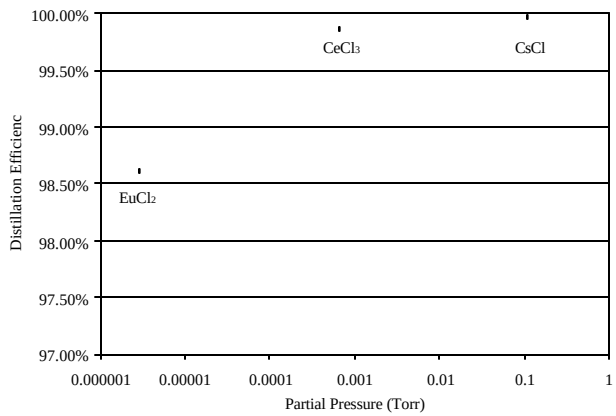

Figure 7: Distillation efficiencies versus partial pressure of $EuCl_2$, $CeCl_3$, and CsCl.

Considering the concentrations of Cs, Ce, and Eu in the Mk-IV electrorefiner salt, Henry's law may be applicable since all their concentrations are less than 1 wt. %, see Figure 3. Henry's law states that the partial pressure of the species is proportional to its mole fraction for dilute solutions:

$$P_i \propto X_i \qquad (3)$$

Now plotting the distillation efficiencies against partial pressures or mole fractions (Figure 8), a correlation is evident and represented by the regressed line. The linearity of the three efficiencies confirms the earlier assumption that the individual distillation efficiencies are constant at the present concentrations.

Assuming the relationship for distillation efficiencies and concentrations is valid for dilute species, other minor chloride species of the system can be modeled based on their

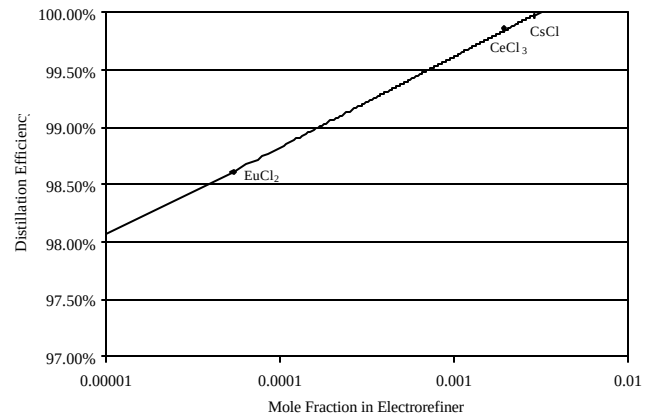

Figure 8: Distillation efficiencies versus mole fraction of $EuCl_2$, $CeCl_3$, and CsCl.

concentrations. Given in Table III are several minor chloride species and their mole fractions in the Mk-IV electrorefiner salt. The actinide chlorides of $NpCl_3$ and $PuCl_3$ are included with the other chlorides of fission products. Using the mole fractions given in Table III and Figure 8, the minor chloride species can be plotted and are shown in Figure 9. All the minor chloride species plotted fall within the mole fractions of $EuCl_2$ and $CeCl_3$ and are tightly grouped in the 0.001 mole fraction region with the exception of $NpCl_3$. Given the placement of the minor chloride species on the line in Figure 9, distillation efficiencies for those species can be interpolated and are included in Table III.

Applying the distillation efficiencies of the minor chloride species in Figure 9, the concentrations of the elements in the uranium product can be calculated and are shown in Figure 10. The expected concentrations of the elements for both the present, after 100 assemblies, as well as the future, end of driver processing, are given. Looking at the present concentrations, it is not surprising that the minor chloride species have not been detected considering the typical analytical limits of quantification. Even for the future concentrations, the minor chloride species will probably not be detected since the concentrations are all less than 10 ppm.

Table III. Characteristics of Minor Chloride Species

Element	Salt Compound	Mole Fraction of Salt Compound	Distillation Efficiency
Np	$NpCl_3$	0.00008	98.74%
Pu	$PuCl_3$	0.00078	99.53%
Ba	$BaCl_2$	0.00122	99.68%
La	$LaCl_3$	0.00104	99.62%
Pr	$PrCl_3$	0.00099	99.61%
Sm	$SmCl_2$	0.00071	99.50%
Sr	$SrCl_2$	0.00115	99.66%
Y	YCl_3	0.00091	99.58%

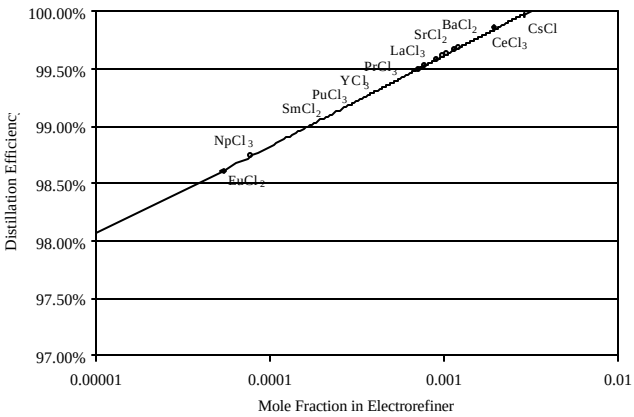

Figure 9: Distillation efficiencies versus mole fraction of minor chloride species.

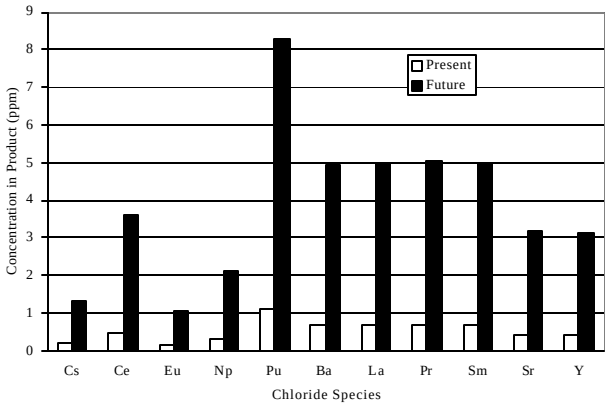

Figure 10: Concentration of minor chloride species in uranium product for both the present and future operations.

Although the present concentrations in the product seem insignificant, a fraction of these elements are radioactive and contribute significantly to the overall activity of the final uranium product, see Table IV. The isotopes of the minor chloride species provide over 2 Ci of activity with a majority provided by the Sr-90.

Table IV. Contribution of Activities for Minor Chloride Species

Salt Compound	Radioactive Isotope	Half-Life (yr)	Specific Activity (Ci/g)	Activity (Ci)	Activity (%)
CsCl	Cs-137	30	87	0.2	9
$EuCl_2$	Eu-155	5	490	0.5	19
$SmCl_2$	Sm-151	93	25	0.1	4
$SrCl_2$	Sr-90	29	138	1.7	68

Conclusions

- Separation of molten salt from uranium during spent fuel treatment operations in the cathode processor has been effective to at least 96% as determined by the distillation efficiencies of selected isotopic tracers.
- Representation of the chloride species of CsCl, $CeCl_3$, and $EuCl_2$ was demonstrated using the isotopic tracers of Cs-137, Ce-144, and Eu-155, respectively.
- Separation of the minor chloride species, including CsCl, $CeCl_3$, and $EuCl_2$, from uranium is dependent on their concentrations in the Mk-IV electrorefiner salt according to Henry's law.
- Other minor chloride species in the system can be modeled based on the distillation efficiencies of CsCl, $CeCl_3$, and $EuCl_2$.
- Distillation efficiencies of the minor chloride species can be used to project the contribution of radioactive nuclides to the activity of the uranium product.

Acknowledgements

The authors would like to acknowledge the Fuel Conditioning Facility operations personnel for their contributions and S.A. Barker, P.J. Crane, D.G. Cummings, R.E. DiFelici, L.E. Foulkrod, and M.T. Sayer for analytical services. Support of this research was by the U. S. Department of Energy under Contract W-31-109-ENG-38.

References

1. B.R. Westphal and R.D. Mariani, "Uranium Processing during the Treatment of Sodium-Bonded Spent Nuclear Fuel," JOM, 52 (9) (2000), 21-25.

2. R.W. Benedict and H.F. McFarlane, "EBR-II Spent Fuel Demonstration Project Status," Radwaste, 5 (1998), 23-30.

3. R.D. Mariani et al., "Selected Uranium Product Characteristics for the EBR-II Spent Fuel Treatment Program," Trans. Am. Nucl. Soc., 77 (1997), 76-78.

4. A.R. Brunsvold, P.D. Roach, and B.R. Westphal, "Design and Development of a Cathode Processor for Electrometallurgical Treatment of Spent Nuclear Fuel," Proc. Eighth Int. Conf. Nucl. Eng. (ICONE), (New York, NY: ASME, 2000).

5. B.R. Westphal, "Distillation Modeling for a Uranium Refining Process," Light Metals 1996, ed. W. Hale (Warrendale, PA: TMS, 1996), 1185-1189.

6. C.E. Crouthamel, Applied Gamma-Ray Spectrometry (Elmsford, NY: Pergamon Press Inc., 1970), 247-250.

7. B.R. Westphal, J.R. Krsul, and D.W. Maddison, "Salt Distillation Efficiencies for Cathode Processing of Spent Nuclear Fuel," Proc. Third Topical Mtg. DOE Spent Nucl. Fuel & Fissile Mtl. Management, (LaGrange Park, IL: ANS, 1998), 676-681.

8. F.H. Spedding and A.H. Daane, ed., The Rare Earths (New York, NY: John Wiley & Sons, Inc., 1961), 6-12.

9. M.C. Sneed and R.C. Brasted, ed., Comprehensive Inorganic Chemistry - Volume Four (Princeton, NJ: D. Van Nostrand Co., Inc., 1964), 164-175.

10. L. Brewer, "The Fusion and Vaporization Data of the Halides," The Chemistry and Metallurgy of Miscellaneous Materials – Thermodynamics, ed. L.L. Quill (New York, NY: McGraw-Hill Book Co., Inc., 1950), 193-219.